CFD SIMULATION OF SAWDUST GASIFICATION

by Fajri Vidian

Submission date: 17-Apr-2023 10:39AM (UTC+0700)
Submission ID: 2066707877
File name: Rahmat_CFD_open_Top.pdf (1.05M)
Word count: 3517
Character count: 17937

ZIBELINE INTERNATIONAL PUBLISHING

Journal of Mechanical Engineering Research and Developments (JMERD)

DOI : http://doi.org/10.26480/jmerd.02.2018.106.110

ISSN: 1024-1752

CODEN : JERDF0

CFD SIMULATION OF SAWDUST GASIFICATION ON OPEN TOP THROATLESS DOWNDRAFT GASIFIER

Fajri Vidian[1]*, Rachmat Dwi Sampurno[1,2], Ismail[3]

[1]Department of Mechanical Engineering, Faculty of Engineering, Universitas Sriwijaya, Jalan Raya Palembang - Prabumulih km 32, Indralaya, Ogan Ilir, Sumatera Selatan 30662, Indonesia,
[2]Magister Student Department of Mechanical Engineering, Faculty of Engineering, Universitas Sriwijaya,
[3]Department of Mechanical Engineering, Faculty of Engineering, Universitas Pancasila, Srengseng Sawah – Jakarta 12640, Indonesia
**Corresponding Author Email: fajri.vidian@unsri.ac.id*

ARTICLE DETAILS

Article History:

Received 3 May 2018
Accepted 5 Jun 2018
Available online 11 July 2018

ABSTRACT

Sawdust is one of alternative energy sources to substitute the fossil fuels. The utilization of sawdust to produce energy can be done through different types of technologies. Gasification is one of techonology that can be used to convert sawdust into energy. Sawdust has the characteristics of small bulk density and bind to one another. The gasifier type corresponding to these properties is an open top throatless downdraft gasifier. The prediction of producer gas composition can be done through a simulation. This study was conducted to obtain the distribution of combustible gas, tar concentration and temperature at the inside of gasifier on different variations of equivalence ratio by using 2D of computational fluid dynamic. Simulation was performed on the variation of equivalence ratio of 0.2, 0.3 and 0.4. The simulation results showed that the increase of equivalence ratio tend to decrease of CO, H_2, CH_4 and tar followed by increasing of temperature at the inside of the gasifier.

KEYWORDS

Open top, Throatless, downdraft gasifier, Gasifications, Sawdust, Computational Fluid Dynamic.

1. INTRODUCTION

Biomass energy has considerable potential in Indonesia. One of the sources of biomass available is sawdust. The sawdust is more accessible in Indonesia with production of 1.4 million m^3/year [1]. Gasification is one method to convert sawdust to energy. The gasification process always take place on equivalence ratio of 0.2 to 0.4 for producing combustible gas (CO, H_2, CH_4), Sawdust have characteristics small bulk density and binding one another, due to its characterics so the open top throtless of downdraft gasifier is very suitable for sawdust gasification [2]. The prediction of combustible gas distribution, temperature distribution and tar distribution at the inside of gasifier is important before the construction and the fabrication of the gasifier. Numerical simulation using CFD is one of popular methods to the prediction it. Many researchers have done the prediction of combustible gas composition using CFD inside downdraft gasifier. CFD simulation on the imbert downdraft gasifier using wood chip as fuel has been done by author, the results showed that the combustible gas in mole fraction were about 38.23% of CO, 23.24% of H_2, and 0.11% of CH_4 at equivalence ratio of 0.24 [3]. Furthermore, the simulation on throatless downdraft gasifier using wood chip as fuel has been done, the results showed that the maximum CO in mole fraction was 20.8% at equivalence ratio about 0.35 and would decrease with increasing of air flow rate (equivalence ratio) [4]. Lignite coal as fuel on imbert downdraft gasifier has been simulated the result showed that the mass fraction of CO about 20 % in pyrolysis zone [5]. Another result CFD simulation on downdraft gasifier was reported with combustible gas composition in mass fraction were about 18.7% of CO, 11.8% of H_2 and 2.58% of CH_4 [6]. The small bulk of density for biomass of risk husk was simulated in imbert downdraft gasifier, the results of combustible gas in mole fraction were about 22% of CO, 13% of H_2 and 1.7% of CH_4 at equivalence ratio of 0.3 [7]. The closed top throatless downdraft gasifier has been simulated using steam air ratio of 0.89 as agent, the results of the simulation were about 40% of CO, 25% of H_2 and 4% of CH_4 [8]. According to the results of CFD simulation before, the results of combustible gas depends on the construction of downdraft gasifier, the used fuel and the equivalence ratio. In this research was done CFD Simulation on gasification process at open top throatless downdraft gasifier using sawdust as fuel. The simulation was done on the variation of equivalence ratio to investigate the distribution of combustible gas composition, the distribution of temperature and the distribution of tar concentration at the inside of gasifier.

2. SIMULATION METHODOLOGY

2.1 Governing Equation

In this simulation Euler – Lagrange approaching were used to treat fluid flow as continuum and particle tract as discrete phase. Several equations have been developed to solve interaction continuum phase and discrete phase in term of gasification process. The fluid flow and reaction were solved using equation of mass, energy, standard k-ε of turbulent and spices transport. The solid movement and its reaction were solved using discrete phase equation, heating equation, devolatisation equation and heat transfer equation; The equations are used as follows:

2.1.1 Mass conservation equation

$$\frac{\partial \rho}{\partial t} + \nabla . (\rho \vec{v}) = S_m \quad (1)$$

2.1.2 Momentum conservation equation

$$\frac{\partial}{\partial t}(\rho \vec{v}) + \nabla(\rho \vec{v} \vec{v}) = -\nabla p + \nabla \bar{\tau} + \rho \bar{g} + \vec{F} \quad (2)$$

2.1.3 Energy conservation equation.

$$\frac{\partial}{\partial t}(\rho E) + \nabla\left(\vec{v}(\rho E + p)\right) = \nabla\left(k_{eff}\nabla T - \sum_j h_j \vec{J}_j + \left(\bar{\bar{\tau}}_{eff}\vec{v}\right)\right) + S_h \quad (3)$$

2.1.3 Turbulence standard k-ε equation

$$\frac{\partial}{\partial t}(\rho k) + \frac{\partial}{\partial x_i}(\rho k u_i) = \frac{\partial}{\partial x_j}\left[\left(\mu + \frac{\mu_t}{\sigma_k}\right)\frac{\partial k}{\partial x_j}\right] + G_k + G_k - \rho\varepsilon - Y_M + S_k \quad (4)$$

$$\frac{\partial}{\partial t}(\rho\varepsilon) + \frac{\partial}{\partial x_i}(\rho\varepsilon u_i) = \frac{\partial}{\partial x_j}\left[\left(\mu + \frac{\mu_t}{\sigma_\varepsilon}\right)\frac{\partial \varepsilon}{\partial x_j}\right] + C_{1\varepsilon}\frac{\varepsilon}{k}(G_k + C_{3\varepsilon}G_b) - C_{2\varepsilon}\rho\frac{\varepsilon^2}{k} + S_\varepsilon \quad (5)$$

2.1.4 Radiative transfer equation

$$\frac{dI(\vec{r},\vec{s})}{ds} + (a+\sigma_s)I(\vec{r},\vec{s}) = an^2\frac{\sigma T^4}{\pi} + \frac{\sigma_s}{4\pi}\int_0^{4\pi} I(\vec{r},\vec{s}')\Phi(\vec{r},\vec{s}')d\Omega' \quad (6)$$

2.1.5 Species transport equation

$$\frac{\partial}{\partial t}(\rho Y_i) + \nabla(\rho\vec{v}Y_i) = -\nabla.\vec{J}_i + R_i + S_i \quad (7)$$

$$R_i = M_{w,i}\sum_{r=1}^{N_R}\hat{R}_{i,r} \quad (8)$$

2.1.6 Finite rate

$$\hat{R}_{i,r} = \Gamma\left(v''_{i,r} - v'_{i,r}\right)\left(k_{f,r}\prod_{j=1}^{N}\left[C_{j,r}\right]^{\eta'_{j,r}} - k_{b,r}\prod_{j=1}^{N}\left[C_{j,r}\right]^{\eta''_{j,r}}\right) \quad (9)$$

$$k_{f,r} = A_r T^{\beta_r} e^{-E_r/RT} \quad (10)$$

$$k_{b,r} = \frac{k_{f,r}}{K_r} \quad (11)$$

2.1.7 Eddy- dissipation rate

$$R_{i,r} = v'_{i,r}M_{w,i}A\rho\frac{\varepsilon}{k}\min_R\left(\frac{Y_R}{v'_{R,r}M_{w,R}}\right) \quad (12)$$

$$R_{i,r} = v'_{i,r}M_{w,i}AB\rho\frac{\varepsilon}{k}\frac{\sum_P Y_P}{\sum_j^N v''_{j,r}M_{w,j}} \quad (13)$$

2.1.8 Particle motion equation

$$\frac{du_p}{dt} = F_D\left(u - u_p\right) + \frac{g_x(\rho_p - \rho)}{\rho_p} + F_x \quad (14)$$

$$F_D = \frac{18\mu}{\rho_p d_p^2}\frac{C_D Re}{24} \quad (15)$$

2.1.9 Particle heating equation

$$m_p c_p\frac{dT_p}{dt} = hA_p\left(T_\infty - T_p\right) + \varepsilon_p A_p\sigma\left(\theta_R^4 - T_p^4\right) \quad (16)$$

2.1.10 Single rate of particle devolatisation equation

$$m_p c_p\frac{dT_p}{dt} = hA_p\left(T_\infty - T_p\right) - \frac{dm_v}{dt}h_{fg} + A_p\varepsilon_p\sigma\left(\theta_R^4 - T_p^4\right) \quad (17)$$

$$-\frac{dm_p}{dt} = k\left[m_p - \left(1 - f_{v,0}\right)\left(1 - f_{w,0}\right)m_{p,0}\right] \quad (18)$$

2.1.11 Multiple surface of particle combustion equation

$$m_p c_p\frac{dT_p}{dt} - hA_p\left(T_\infty - T_p\right) - f_h\frac{dm_v}{at}H_{reac} + A_p\in_p\sigma\left(\theta_R^4 - T_p^4\right) \quad (19)$$

Particle species j(s) + gas phase species n → products (20)

$$\bar{R}_{j,r} = A_p\eta_r Y_j R_{j,r} \quad (21)$$

Gasification reaction involved the kinetic reactions of devolatisation, reduction and combustion. Devolatisation of volatile equation (R1) has been developed base on the main composition product the volatile pyrolysis were CO, CO_2, H_2, CH_4, H_2O and tar with ignored the composition of NH_3 and H_2S [8]. The tar cracking equation (R8) has been adopted from [9]. The gasification reactions are used as shown in Table 1. The kinetic controlled gasification reactions are summarized in Table 2.

Table 1: Gasification Reaction

	Reaction	
R1	Volatile → 0.268 CO + 0.295 CO_2 + 0.5 H_2 + 0.094 CH_4 + 0.255 H_2O + 0.2 Tar	(23)
R2	C(s) + 0.5 O_2 → CO	(24)
R3	C(s) + H_2O → CO + H_2	(25)
R4	C(s) + CO_2 → 2CO	(26)
R5	C(s) + 2H_2 → CH_4	(27)
R6	CO + H_2O → CO_2 + H_2	(28)
R7	CH_4 + H_2O → CO + 3H_2	(29)
R8	Tar → 0.22 tar inert + 0.563 CO + 0.111 CO_2 + 0.017 H_2 + 0.088 CH_4 + 0.255 H_2O	(30)
R9	CO + 0.5 O_2 → CO_2	(31)
R10	2H_2 + O_2 → 2 H_2O	(32)
R11	CH_4 + 1.5 O_2 → CO + 2H_2O	(32)

Table 2: The kinetic of reactions

	A (consisten Unit)	E (J/kmol)	References
R1	5.7e+05	8.1e+07	[10]
R2	8.91e+03	1.4974e+08	[11]
R3	1.517e+08	1.2162 e+08	[10],[12]
R4	36.16	7.739e+07	[10],[12]
R5	4.189e-03	1.921e+07	[10],[12]
R6	1.389e+03	1.256e+07	[13],[14]
R7	1.65e+11	3.29e+08	[13],[15]
R8	7e+03	8.36e+07	[16],[17]
R9	4.4e+11	1.2552e+08	[13],[18]
R10	3.53e+08	3.05e+07	[4],[8]
R11	9.2e+06	8e+07	[13], [19]

2.2 Computational Model

The gasifier was modeled with 60 cm of height and 20 cm of diameter. Fuel and air were entered from the top of gasifier with hole diameter each of 20 cm and 2 cm respectively as shown in Figure 1. The simulation was conducted on 2D using Ansys Fluent 15. The construction of the gasifier could be divided into two part with the same size and shape. For simplifing process, the simulation was done using axisymmetric condition.

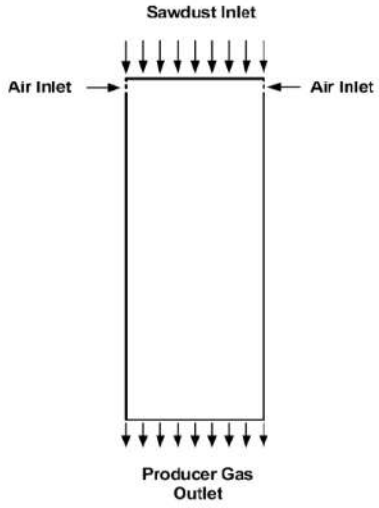

Figure 1: The open top throatless downdraft gasifer

The mass flow of air gasification was calculated base on ultimate analysis of fuel. The volatile and combustible fraction of fuel were based on proximate analysis as shown in Table 3. The boundary condition of simulation is summarized in Table 4

Table 3: The analysis of ultimate and proximate [20]

Description	value
Ultimate	
Carbon	47.45
Hydrogen	6.46
Oxigen	45.54
Nitrogen	0.05
Sulfur	0.12
Proximate	
Moisture	6.75
Ash	0.38
Volatile	80.11
Fixed Carbon	12.76

Table 4: The boundary condition

Parameter	Value
Inlet mass flow of fuel	6 kg/h
Inlet mass flow of air at equivalence ratio (ER) of 0.2	6.9 kg/h
Inlet mass flow of air at equivalence ratio (ER) of 0.3	10.35 kg/h
Inlet mass flow of air at equivalence ratio (ER) of 0.4	13.8 kg/h
Inlet temperature of fuel	499 K
Inlet temperature of air	300

3. RESULTS AND DISCUSSION

The Effect of Equivalence Ratio on The distribution of Combustible Gas Composition at The inside of Gasifier. Figure 2, 3, and 4 shows the increasing of equivalence ratio tended to decrease the distributions of CO, H_2 and CH_4 at the inside of gasifier were presented on decreasing of the area of yellow and cyan color. The higher composition of combustible gas concentrated in the middle of gasifier caused by the effect of the air inlet pushed tracking particle to the center of the gasifier. Therefore,the gasification reactions become more dominant in this zone. The combustible gas at point of air inlet had lower concentration caused by the spices needed time and space for reaction of gasification [21]. The combustible concentration was higher at the top of gasifier, indicating the reaction combustion of combustible gas (R9, R10, and R11) increased from top to down of gasifier.

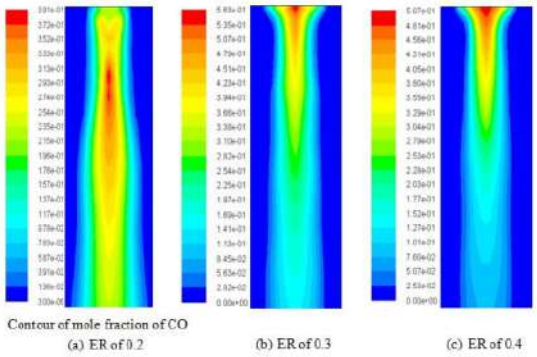

Figure 2: The distribution of CO compositions

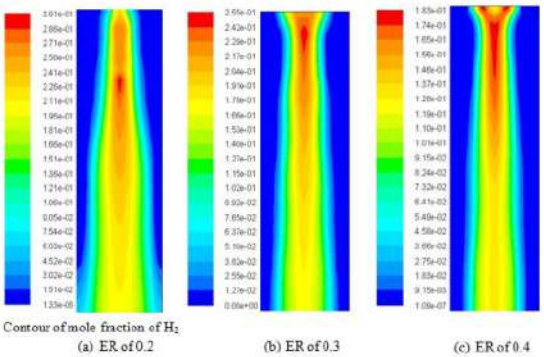

Figure 3: The distribution of H_2 compositions

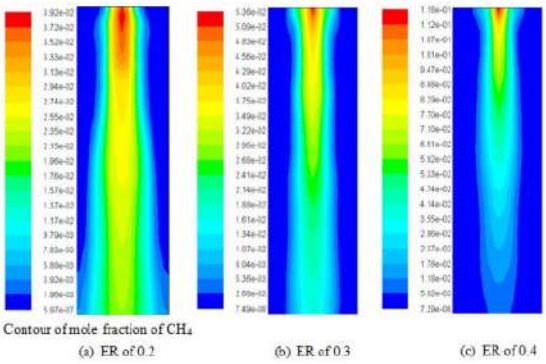

Figure 4: The distribution of CH_4 compositions

The final composition of the combustible gas at the center of outlet gasifier as shown in Figure 5. It was found that as the equivalence ratio increased, the composition of CO, H_2 and CH_4 decreased from 24 % to 10% (CO), 21% to 14% (H_2), 2.2% to 1.2% (CH_4), the behaviors of combustible gas composition have the same trends as mentioned by [4, 12]. This is due to the increase of combustion reaction of combustible gas (R9,R10,R11). Furthermore, the increasing of CO combustion (R9) contributed to the increase of the concentration of CO_2 from 16% to 20%. The N_2 concentration tended to increase from 41% to 55% due to the rise of air in which N_2 is main component of air. The composition of CO and H_2 in every point of equivalence ratio was quite similar. This was due to the fact that more H_2O from evaporation reacted with CO to increase H_2 concentration, indicating the same trend to the experiment at open top throatless downdraft gasifier [22-24]. The comparison of simulation with the experimental resulted at equivalence ratio about 0.2 is shown in Figure 6 [22]. The results showed similar agreement with this experiment.

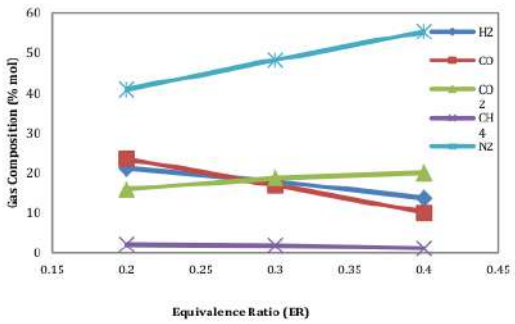

Figure 5: The effect of equivalence ratio on gas composition

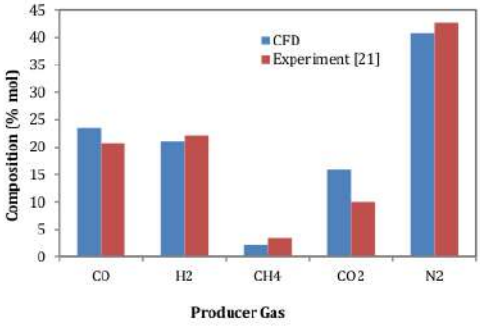

Figure 6: The comparation between of CFD and Experiment

The Effect of Equivalence Ratio on The distribution of Temperature at The inside of Gasifier. Figure 7 shows the increasing of equivalence ratio tended to increase the temperature distribution at the inside of gasifier, especially in the centre of the gasifier as represented by decreasing of cyan color and increasing of yellow color. It was caused by the more of combustible gas (CO, H_2 and CH_4) in this location as shown in Figure 2,3 and 4 contacted with more of air for the combustion reaction. At the top of gasifier, the temperature distribution was lower than the bottom caused by evaporation and devolatisation process that absorbed heat more dominance. The increasing of the temperature distribution at the inside of the gasifier further lead to an increase on the temperature at centre outlet of the gasifier from 1251 K to 2241 K.

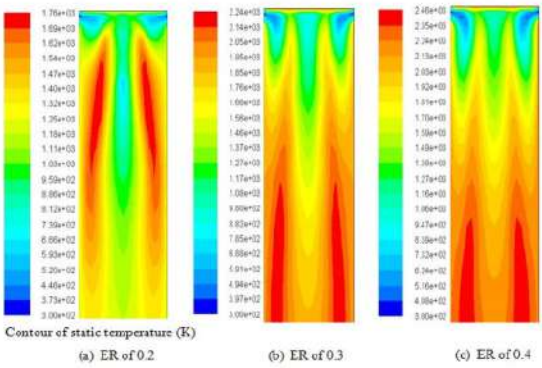

Figure 7: The distribution of temperature

The Effect of Equivalence Ratio on The distribution of Tar Concentration at The inside of Gasifier. Figure 8 shows the increasing of equivalence ratio tended to decrease the distribution of tar concentration inside of the gasifier as represented by decreasing the area of cyan and yellow color at inside of the gasifier, due to higher cracking of the tar (R8) was contributed by increasing of temperature at the inside of gasifier as shown in Figure 7. The tar concentration was higher at the top of gasifier was contributed by the lower temperature at this zone. The final concentration of tar decreased from 0.37 % to 0.29% for increasing of equivalence ratio from 0.2 to 0.4 at the centre outlet of gasifier. Decreasing of tar was followed by appearing tar inert as shown in Figure 9. The concentration tar inert at the inside of gasifier decreased with increasing of equivalence ratio as represented by decreasing the area of yellow and red color. The final concentration of the tar inert decreased from 1.11% to 0.82% for increasing of equivalence ratio from 0.2 to 0.4 at the centre outlet of gasifier, because of the tar inert is a conversion of the tar, as explained by equation R8, This result have same trend with reporting [8].

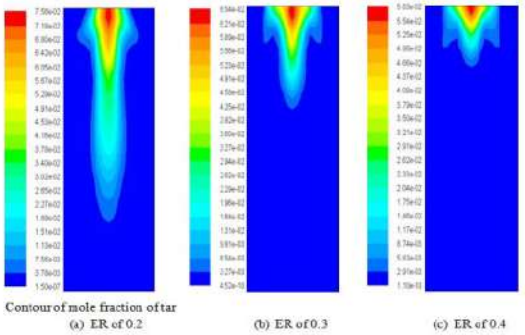

Figure 8: The distribution of tar compositions

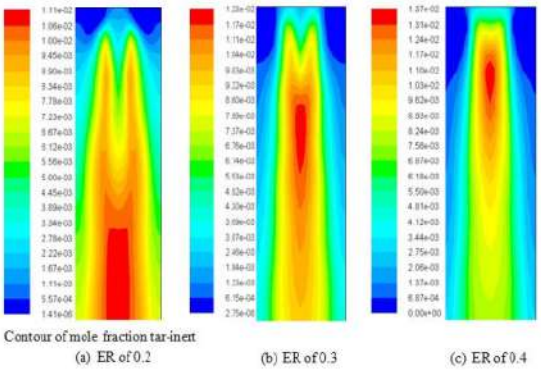

Figure 9: The distribution of tar-inert compositions.

4. CONCLUSIONS

In this research, open top throatless downdraft gasifier has been simulated using CFD to investigate effect equivalence ratio each of 0.2, 0.3 and 0.4 on the distribution of gas composition, temperature and tar concentration. The increasing of equivalence ratio tended to decrease distribution of combustible gas (CO, H_2, CH_4) composition and tar concentration followed by increasing of temperature distribution at the inside of gasifier. In each equivalence ratio, the combustible gas composition decreased from the top to the bottom of the gasifier as well as the tar concentration, otherwise for the temperature distribution increased from the top to the bottom of gasifier. The maximum of final of combustible gas composition at the center of outlet gasifier each of CO 24%, H_2 21% CH_4 22% were resulted on equivalence ratio of 0.2. The minimum of tar concentration of 0.29% and the maximum of temperature of 2241 K were existed on equivalence ratio of 0.4 at the center of outlet gasifier.

REFERENCES

[1] Usman, M. 2013. Alternatif pemanfaatan limbah industri pengolahan kayu sebagai arang briket. Jurnal APTEK, 5 (1), 1-10.

[2] Martínez, J.D., Mahkamov, K., Andrade, R.V., Lora, E.E.S. 2012. Syngas production in downdraft biomass gasifiers and its application using internal combustion engines. Renewable Energy, 28, 1-9.

[3] Janajreh, I., Shrah, M.A. 2012. Numerical and experimental investigation of downdraft gasification of wood chips. Energy Conversion and Management, 65, 783-792.

[4] Meenaroch, P., Kerdsuwan, S., Laohalidanond, K. 2015. Development of kinetics models in each zone of a 10 kg/hr downdraft gasifier using computational fluid dynamics. Energy Procedia, 79, 278 – 283.

[5] Patel, K.D., Shah, N.K., Patel, R.N. 2013. CFD analysis of spatial distribution of various parameters in downdraft gasifier. Procedia Engineering, 51, 764-769.

[6] Chodapaneedi, R., Sanke, N., Reddy, D.D.N. 20133. CFD simulation of an advanced biomass gasifier. IOSR Journal of Mechanical and Civil Engineering, 42-48.

[7] Murugan, P.C., Sekhar, J.S. 2017. Species - transport cfd model for the gasification of rice husk (oryza sativa) using downdraft gasifier. Computers and Electronics in Agriculture, 139, 33–40.

[8] Wu, Y., Zhang, Q., Yang, W., Blasiak, W. 2013. Two-dimensional computational fluid dynamics simulation of biomass gasification in a downdraft fixed-bed gasifier with highly preheated air and steam. Energy and Fuels, 27, 3274-3282.

[9] Wurzenberger, J.C., Wallner, S., Raupenstrauch, H., Khinast, J.G. 2002. Thermal conversion of biomass: comprehensive reactor and particle modelling. AIChE Journal, 48 (10), 2398-2411.

[10] Gao, N., Li, N. 2008. Modeling and simulation of combined pyrolisis and reduction zone for a downdraft biomass gasifier. Energy Conversion and Management, 49, 3483-3490.

[11] Zhou, W., Zhao, C.S., Duan, L.B., Qu, C.R., Chen, X.P. 2011. Two-dimensional computational fluid dynamics simulation of coal combustion in a circulating fluidized bed combustor. Chemical Engineering Journal, 166, 306-314.

[12] Wang, W., Kinoshita, C.M. 1993. Kinetic model of biomass gasification. Solar Energy, 51 (1), 19-25.

[13] Su, Y., Luo, Y., Chen, Y., Wu, W., Zhang, Y. 2011. Experimental and numerical investigation of tar destruction under partial oxidation environment. Fuel Processing Technology, 92, 1513–1524.

[14] Biba, V., Macak, J., Klose, E., Malecha, J. 1978. Mathematical model for the gasification of coal under pressure. Industrial & Engineering Chemistry Process Design and Development, 17, 92–98.

[15] Andreas, J. 1995. Reaktionskinetische untersuchungen zur thermischen zersetzung von modellkohlenwasserstoffen. Erdol Erdgas Kohle, 111, 479–484.

[16] Fagbemi, L., Khezami, L., Capart, R. 2001. Pyrolysis products from different biomasses: application to the thermal cracking of tar. Applied Energy, 69, 293 – 306.

[17] Scott, D.S., Piskorz, J., Radlein, D. 1985. Liquid product from the continuous flash pyrolysis of biomass. Industrial & Engineering Chemistry Process Design, 24, 581–588.

[18] Jones, W.P., Lindstedt, R.P. 1998. Global reaction schemes for hydrocarbon combustion. Combustion and Flame, 73, 233–249.

[19] Bryden, K.M., Ragland, K.W. 1996. Numerical modelling of deep, fixed bed combustor. Energi and Fuel, 10, 269 – 275.

[20] Vidian, F., Basri, H., Surjosatyo, A. 2017. Experiment on sawdust gasification using open top downdraft gasifier incorporated with internal combustion engine. ARPN Journal of Engineering and Applied Sciences, 12 (4), 1152-1156.

[21] Luan, Y.T., Chyou, Y.P., Wang, T. 2013. Numerical analysis of gasification performance via finite rate model in a cross -type two-stage gasifier. International Journal of Heat and Mass Transfer, 57, 558-566.

[22] Kuhe, A., Aliyu, S.J. 2015. Gasification of 'loose' groundnut shells in throatless downdraft gasifier. International Journal of Renewable Energy Development, 4 (2), 125-130.

[23] Gnanendra, P.M, Rajan, N.K.S. 2016. Experimental Study on Performance of Downdraft Gasifier Reactor Under Varied Ration of Secondary and Primary Air Flows. Energy Procedia, 90, 38-49.

[24] Prando, D., Ail, S.S., Chiaramonti, D., Barratieri, M., Dassapa, S. 2016. Characterisation of the producer gas from an open top gasifier: Assessment of different tar analysis approaches. Fuel, 81, 566-572.

CFD SIMULATION OF SAWDUST GASIFICATION

ORIGINALITY REPORT

11%	10%	10%	%
SIMILARITY INDEX	INTERNET SOURCES	PUBLICATIONS	STUDENT PAPERS

MATCH ALL SOURCES (ONLY SELECTED SOURCE PRINTED)

3%

★ up2m-ft.univpancasila.ac.id

Internet Source

Exclude quotes	On	Exclude matches	< 1%
Exclude bibliography	On		